Transition Metal Chemistry **29**: 623–629, 2004.

Synthesis, spectral, electrochemical and magnetic properties of new asymmetric dicopper(II) complexes bearing chemically distinct coordination sites

Rajaram Mahalakshmy, Rangarajan Venkatesan and Pillutla Sambasiva Rao*
Department of Chemistry, Pondicherry University, R.V. Nagar, Kalapet, Pondicherry 605 014, India

Ramu Kannappan
Leiden Institute of Chemistry, Gorlaeus Laboratories, Leiden University, P.O. Box 9502, 2300, RA, Leiden, The Netherlands

Thekkel Madan Rajendiran
Department of Biological Chemistry, University of Michigan Medical School, MSB I, Ann Arbor, MI 48109-0606, USA

Received 14 January 2004; accepted 02 March 2004

Abstract

Two new unsymmetrical binucleating ligands, 2-[bis(3-*N*,*N*-dimethylaminopropyl)-aminomethyl]-6-[prolin-1-yl)methyl]-4-bromophenol [H_2L^1] and 2-[bis(3-*N*,*N*-dimethylaminopropyl)aminomethyl]-6-[prolin-1-yl)methyl]-4-methylphenol [H_2L^2], and their dicopper(II) complexes with different exogenous bridging motifs (OAc, Br and Cl) have been prepared and characterized by spectral, electrochemical, magnetic and e.p.r. studies. Electrochemical studies indicate the presence of two irreversible reduction peaks in the cathodic region. Variable temperature magnetic susceptibility studies of the complexes show that the extent of antiferromagnetic coupling increases in the order: $OAc^- < Cl^- < Br^-$. Broad isotropic or axial symmetric spectral features are observed in powder e.p.r. spectra of the complexes at 77 K. A comparison of the electrochemical and magnetic behaviour of the complexes derived from the ligands is discussed on the basis of an exogenous bridge as well as the substituent at the *para* position of the phenolic ring.

Introduction

The chemistry of dinucleating ligands that provide chemically distinct donor sets is of current interest to bioinorganic chemists [1–3]. Ligands of this type readily form dinuclear transition metal complexes in which the metal ions are often found in chemically or geometrically distinct environments similar to that found in the active site structure of haemocyanin and tyrosinase. The unsymmetrical nature of the dicopper site in haemocyanin is demonstrated in the X-ray crystal structure of oxyhaemocyanin [4, 5] and sequence homology studies on tyrosinases have shown that whilst one of the copper sites is highly conserved, the structure of the second copper site is quite variable [5]. This observation led to the suggestion that unsymmetrical dinucleating ligands are beacons for modeling the active site structure of dinuclear metallo biosites existing in biological systems.

In the present work, two new unsymmetrical binucleating ligands have been synthesized *via* a sequential aromatic Mannich base reaction using *para* substituted phenols, paraformaldehyde, a secondary amine and L-proline. Preparation, spectral, electrochemical, magnetic and e.p.r. properties of dinuclear copper(II) complexes $[Cu_2L(X)]^+$ with different exogenous bridging motifs (X = OAc, Br and Cl) of these ligands are herein reported.

Experimental

Physical measurements

I.r. spectra were recorded on a Perkin–Elmer IR 598 spectrophotometer on a KBr disk in the 4000–250 cm^{-1} range. ^{1}H-n.m.r. (400 MHz) and ^{13}C-n.m.r. (100 MHz) spectra were recorded using a model JEOL FX–400 FT-n.m.r. spectrometer in $CDCl_3$ solution with $SiMe_4$ as internal standard. Elemental (C, H, N) analyses were determined using a Heraus rapid analyzer. Cu was estimated by AAS using a model 2380 Perkin-Elmer spectrophotometer. Electron impact (EI) mass spectra were recorded on a JEOL D-300 mass spectrometer. Fast atom bombardment (FAB) mass spectra were recorded on a JEOL SX 102/DA-6000 mass spectrometer using Ar/Xe (6 kV, 10 mA) as the FAB gas and *meta*-nitrobenzyl alcohol was used as the matrix (NBA). Electronic spectral studies were conducted on an Ocean

*Author for correspondence

Optics SD1000 miniature fiber optics Spectrometer using a 1 cm quartz cuvette in the 200–800 nm wavelength range. Molar conductance (Λ_m) values were measured using a control dynamics conductivity-meter in DMF solvent. The electrochemical measurements were performed at room temperature in DMF, under O_2-free conditions, using an Autolab PGSTAT 12 controlled by General Purpose Electrochemical system Software (GPES). A three-electrode assembly comprising a Pt disc-working electrode, a Pt rod auxiliary electrode and a saturated calomel reference electrode (SCE) was used. The supporting electrolyte was *n*-Bu_4NClO_4 (TBAP) (0.1 mol) and all solutions were in *ca.* 10^{-3} mol concentration. Magnetic susceptibility data of the powdered samples were measured in the 80–300 K range using a Princeton Applied Research Model 155 VSM instrument operating at a 5000 G magnetic field. The instrument was calibrated using metallic Ni. Diamagnetic corrections were evaluated using Pascal's constants. e.p.r. spectra were recorded with a JEOL TES100 e.p.r. spectrometer. Low temperature measurements were recorded at the liquid N_2 temperature (77 K) using ES-UCD3X insertion type Dewar.

Materials

All chemicals and reagents were obtained from commercial sources and were used without further purification. The solvents for electrochemical measurements, ligands and complex synthesis were purified and dried according to the standard procedure [6]. *n*-Bu_4NClO_4, used as the supporting electrolyte for electrochemical measurements, was prepared from *n*-Bu_4NBr, $HClO_4$ and $NaHCO_3$. Recrystallisation was performed from hot EtOH and further drying was carried out in a vacuum desiccator.

Synthesis of ligands

2-{[Bis-(3-dimethylaminopropyl)-amino]-methyl}-4-bromophenol [PC-I]

To 3,3-iminobis(*N*,*N*-dimethylpropylamine) (0.021 mol, 3.93 g), was added paraformaldehyde (0.021 mol, 0.63 g). After the reaction mixture has been stirred for 1 h at 60 °C, *p*-BrC_6H_4OH (0.020 mol, 7.45 g), dissolved in EtOH, was added and the mixture was boiled under reflux for 20 h. The EtOH was removed under reduced pressure to give a viscous yellow oil, which was washed well with aq.Na_2CO_3 and extracted with CH_2Cl_2. The organic layers were collected, dried over anhydrous Na_2SO_4, and evaporated to leave a crude oil which was purified further by column chromatography on neutral alumina (CH_2Cl_2/MeOH, 9:1) to give the product as a pale yellow oil. Yield: 75% (5.58 g). ^{1}H-n.m.r. (400 MHz): δ 1.69 (q, 4H); 2.19 (s, 12H); 2.25 (t, 4H); 2.55 (t, 4H); 3.70 (s, 2H); 6.68 (d, 1H); 7.06 (s, 1H); 7.24 (d, 1H). ^{13}C-n.m.r. (100 MHz): 26.15 (t); 44.45 (q); 47.29 (t); 50.72 (t); 56.44 (t); 109.58 (s); 117.07 (d); 123.63 (s); 130.27 (d); 131.40 (d); 156.64 (s). $m/z = 372$ (M^+).

2-{[Bis-(3-dimethylaminopropyl)-amino]-methyl}-4-methylphenol [PC-II]

Following the procedure for PC-I, reaction of 3,3-iminobis(*N*,*N*-dimethylpropylamine) (0.021 mol, 3.93 g), paraformaldehyde (0.021 mol, 0.63 g) and *p*-cresol (0.020 mol, 2.16 g) in EtOH, after 20 h, workup, and chromatographic separation on alumina (CH_2Cl_2/MeOH, 9:1), gave the product as a pale yellow oil. Yield: 72% (4.43 g). ^{1}H-n.m.r (400 MHz): δ 1.61 (q, 4H); 2.10 (s, 12H); 2.12 (t, 4H); 2.16 (s, 3H); 2.46 (t, 4H); 3.60 (s, 2H); 6.61(d, 1H); 6.66 (d, 1H); 6.85 (d, 1H). ^{13}C-n.m.r (100 MHz): 19.98 (q); 23.91(t); 44.83 (q); 50.99 (t); 56.90 (t); 57.67 (t); 115.22 (d); 121.21(s); 127.30 (d); 128.45 (d); 129.39 (s); 155.05 (s). $m/z = 307$ (M^+).

2-[Bis(3-N,N-dimethylaminopropyl)aminomethyl]-6-[(prolin-1-yl)methyl]-4-bromophenol [H_2L^1]

To PC-I (0.010 mol, 3.72 g) in EtOH (50 ml) was added an EtOH solution of L-proline (0.010 mol, 1.15 g) followed by slow addition of 37% formalin (0.015 mol, 1.2 cm^3). The resulting mixture was stirred at room temperature for 1 h and heated to reflux for 24 h. The solvent was then evaporated to give a yellow oil. Column chromatographic separation on alumina gave the product as a slightly yellow oil. Yield: 42% (2.09 g). ^{1}H-n.m.r (400 MHz): δ 1.67–1.72 (m, 4H, 4H); 2.18 (m, 12H, 2H); 2.49–2.57 (m, 8H); 3.11(t, 1H); 3.63 (s, 2H); 3.70 (s, 2H); 6.68 (s, 1H); 7.06 (s, 1H). ^{13}C-n.m.r (100 MHz): 23.05(t), 24.28 (t), 29.70 (t), 45.26 (q), 47.72 (t), 51.45 (t), 52.99 (t), 55.25 (t), 57.24(t), 67.85(d), 110.50(s), 124.14(s), 126.57(s), 130.91(d), 131.19(d), 157.14 (s), 179.76 (s). $m/z = 499$ (M^+).

2-[Bis(3-N,N-dimethylaminopropyl)aminomethyl]-6-[(prolin-1-yl)methyl]-4-methylphenol [H_2L^2]

The procedure for the synthesis was analogous to that used for H_2L^1, employing PC-II (0.010 mol, 3.07 g), L-proline (0.010 mol, 1.15 g) and formalin (0.015 mol, 1.2 cm^3). Yield: 41% (1.78 g). ^{1}H-n.m.r (400 MHz): δ 1.63–1.75 (m, 4H, 2H); 1.85 (q, 2H); 2.24-2.28 (m, 12H, 2H); 2.29 (s, 3H); 2.51(m, 8H); 3.18 (t, 1H); 3.67 (s, 2H); 3.71(s, 2H); 6.81 (s, 1H); 6.97 (s, 1H). ^{13}C-n.m.r (100 MHz): 20.4 (q), 23.0 (t), 24.3 (t), 29.6 (t), 45.2 (q), 47.5(t), 51.4(t), 51.7(t), 57.3 (t), 57.6 (t), 68.3 (d), 121.7 (s), 123.8 (d), 127.7 (s), 128.8 (d), 129.9 (s), 155.4 (s), 179.1 (s). $m/z = 434$ (M^+).

Synthesis of binuclear copper(II) complexes

[$Cu_2L^1(OAc)$] $BPh_4 \cdot MeOH \cdot H_2O$ (1a)

To a magnetically stirred solution of H_2L^1 (0.001 mol, 0.49 g) in MeOH (25 cm^3) was added drops of Et_3N (0.002 mol, 0.28 cm^3), followed by sequential addition of a MeOH solution of $Cu(OAc)_2 \cdot H_2O$ (0.002 mol, 0.39 g) and $NaBPh_4$ (0.001 mol, 0.34 g) affording a green precipitate. This was refluxed for 3 h, cooled and left to dry in air at room temperature. The green compound, thus obtained, was purified by stirring in hot DMF for 2 h, followed by filtration, washing with

Et_2O and drying in vacuum to give a pure product. Yield: 48%. $C_{50}H_{66}BN_4O_7BrCu_2$ calcd.: C, 57.0; H, 6.3; N, 5.3. Found: C, 57.0; H, 6.3; N, 5.3%. Selected i.r. (KBr) data (ν/cm^{-1}): 3425, 1622, 1580, 1450, 735, 450, 248.

[Cu_2L^2 (OAc)]BPh_4 · MeOH · H_2O (2a)

The complex was synthesized by the procedure used for *(1a)*, but H_2L^2 was used instead of H_2L^1. Yield: 52%. $C_{51}H_{69}BN_4O_7Cu_2$ calcd.: C, 62.0; H, 7.0; N, 5.7. Found: C, 62.0; H, 7.0; N, 5.6%. Selected i.r. (KBr) data (ν/cm^{-1}): 3435, 1632, 1583, 1470, 755, 493, 240. FAB mass, m/z 987 (M^+) [Cu_2L^2(OAc)]BPh_4·MeOH·H_2O, 937 [Cu_2L^2(OAc)]BPh_4, 815 [(M^+)—(Cu+OAc+MeOH · H_2O)], 618 [Cu_2L^2 (OAc)]$^+$.

[Cu_2L^1(Br)]BPh_4·MeOH(1b)

The complex was synthesized by following the procedure described for *(1a)*, using $CuBr_2$ instead of $Cu(OAc)_2 \cdot H_2O$. Yield: 56%. $C_{48}H_{61}BN_4O_4Br_2Cu_2$ calcd.: C, 54.6; H, 5.8; N, 5.3. Found: C, 54.6; H, 5.8; N, 5.3%. Selected i.r. (KBr) data (ν/cm^{-1}): 3397, 1614, 648, 488, 249. FAB mass, m/z 1058 (M+2) [Cu_2L^1(Br)]BPh_4·MeOH, 1026 [Cu_2L^1(Br)]BPh_4, 707 [Cu_2L^1(Br)]$^+$, 628 [Cu_2L^1]$^{2+}$.

[Cu_2L^2(Br)]BPh_4 · MeOH(2b)

The complex was prepared by following the procedure for *(1b)*, but H_2L^2 was used instead of H_2L^1. Yield: 49%. $C_{49}H_{64}BN_4O_4BrCu_2$ calcd.: C, 59.4; H, 6.5; N, 5.7. Found: C, 59.3; H, 6.5; N, 5.6%. Selected i.r. (KBr) data (ν/cm^{-1}): 3445,1629, 674, 493, 240.

[Cu_2L^1(Cl)]BPh_4 · MeOH · H_2O(1c)

The complex was synthesized by following the procedure described for *(1a)*, using $CuCl_2$, instead of $Cu(OAc)_2 \cdot H_2O$. Yield: 49%. $C_{48}H_{63}BN_4O_5BrClCu_2$ calcd.: C, 56.0; H, 6.2; N, 5.4. Found: C, 55.9; H, 6.1; N, 5.4%. Selected i.r. (KBr) data (ν/cm^{-1}): 3345, 1626, 648, 450, 241. FAB mass, m/z 1029 (M^+) [Cu_2L^1(Cl)]BPh_4 · MeOH · H_2O, 979 [Cu_2L^1(Cl)]BPh_4, 660 [Cu_2L^1(Cl)], 625 [Cu_2L^1].

[Cu_2L^2(Cl)]BPh_4 . MeOH · H_2O(2c)

The complex was synthesized by following the procedure for *(1c)*, but using H_2L^2 instead of H_2L^1. Yield: 52%. $C_{49}H_{66}BN_4O_5ClCu_2$ calcd.: C, 61.0; H, 6.9; N, 5.8. Found: C, 61.0; H, 6.8; N, 5.7%. Selected i.r. (KBr) data (ν/cm^{-1}): 3440, 456, 269, 705.

Results and discussion

Synthesis and characterization

Two new unsymmetrical binucleating ligands H_2L^1 and H_2L^2 were synthesized *via* the aromatic Mannich base reaction using *para* substituted phenol, formaldehyde, secondary amine and L-proline. A series of binuclear copper(II) complexes with different exogenous bridging motifs, *viz*. OAc, Br and Cl were synthesized by adding a 2:1 ratio of the corresponding metal salts and ligands (Scheme 1).

The structure of the complexes was elucidated using spectroscopic techniques such as i.r, u.v.–vis., elemental analysis and FAB mass spectrometry. The spectral and

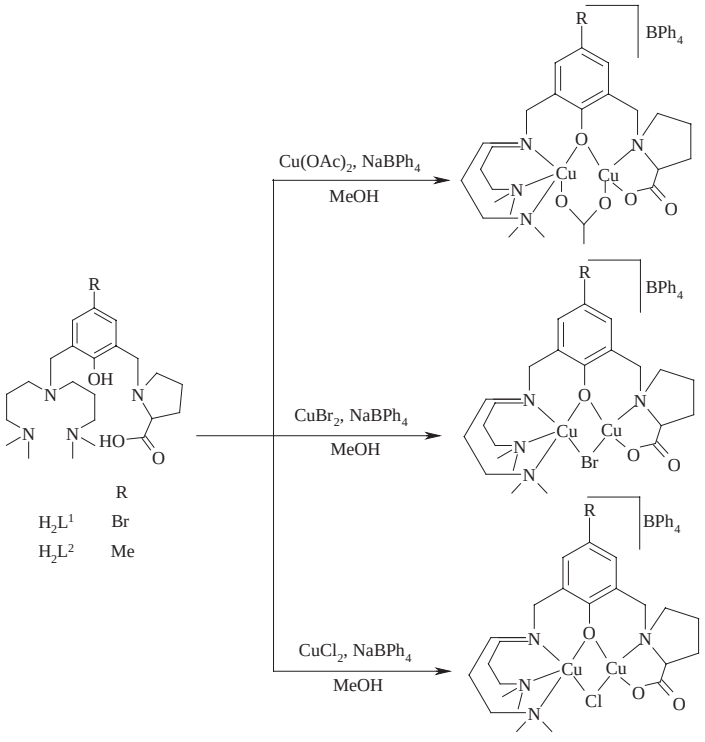

Scheme 1.

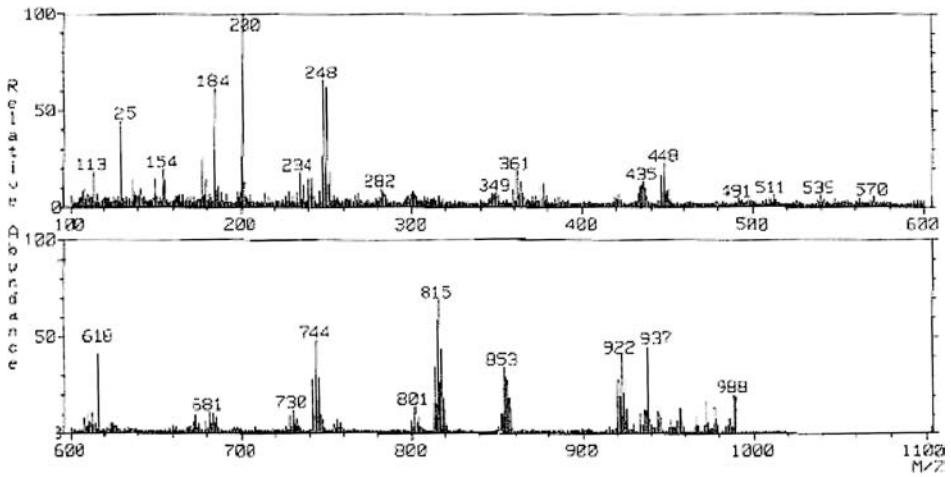

Fig. 1. FAB mass spectrum of complex *(2a)*.

analytical data are given in the experimental section. The FAB mass spectrum of complex *(2a)* is displayed in Figure 1.

Electronic spectra of the complexes were recorded in DMF and the data are given in Table 1. The complexes show three main features: a weak broad band in the 640–700 nm region for the d–d transition, a moderately intense band in the 340–425 nm region for the phenolato-to-copper charge-transfer transition, and a more intense band at *ca.* 220–250 nm for the intraligand π–π^* charge-transfer transition. The position of the phenolato-to-copper LMCT charge-transfer band is sensitive to the electron density on the central copper [7] atom. This peak, observed at a slightly lower wavelength for complexes of H_2L^1, where the *para* position of the phenolic ring is substituted by the electron withdrawing –Br group, increases the Lewis acidity of the copper center, thus shifting the phenolato to copper LMCT band to higher energy [8], whereas for the complexes of H_2L^2, the electron donating –Me group at the *para* position of the phenolic ring, decreases the Lewis acidity of the copper and hence shifts the LMCT band to the lower energy region. Moreover, this band is an exogenous bridging ligand dependent upon and shifting to lower energy for larger X, following the order: OAc < Br < Cl. Absorptions due to $X = Cl^-$, Br^- coordination are either weak or absent.

The nature of the bridging mode of the exogenous bridge with the copper ion is determined from i.r. spectral data. The ν_{as}(COO) and ν_s(COO) modes of the acetate complexes *(1a)–(2a)* are seen at 1580, 1450 and 1583, 1470 cm^{-1}, respectively. The small separation between the two vibrations $\Delta\nu_{(asy\text{-}sym)}$ (<150 cm^{-1}) is in accord with the bridging mode of the acetate group [9]. All the complexes exhibit a sharp band at *ca.* 750 cm^{-1} indicating the presence of the counter ion, BPh_4^-. The characteristic Cu—O, Cu—N, Cu—Cl and Cu—Br vibrations [10] for the complexes are observed as sharp peaks at *ca.* 490, 240, 310, 330 cm^{-1}, respectively.

Electrochemistry

Conductivity measurements of binuclear copper(II) complexes in DMF resulted in Λ_m values in the 40–46 Ω^{-1} cm^2 mol^{-1} range, which indicates that they are of the 1:1 electrolyte type (Table 2).

The electrochemical properties of the binuclear copper(II)–copper(II) compounds *(1a)*–*(2c)* were studied by cyclic voltammetry in DMF solution. The cyclic voltammogram of complex *(2c)* is shown in Figure 2. The cyclic voltammograms of all the studied complexes reveal the presence of irreversible cathodic reduction peaks in the −0.30 to −1.81 V range, as is evident from the fact that the shape and position of a reduction peak

Table 1. Electronic absorption and magnetic data of the complexes

Complex	λ_{max}/nm (ε/mol^{-1} cm^{-1})		−2*J*	μ_{eff} per Cu atom (B.M.)	
	d–d	CT	(cm^{-1})	77 K	298 K
(1a)	690 (197)	390, 306, 227	–	–	–
(2a)	699 (78)	425, 332, 245	70	1.17	1.58
(1b)	668 (120)	383, 311, 226	94	1.10	1.68
(2b)	636 (295)	389, 333, 230	–	–	–
(1c)	659 (371)	366, 338, 264	90	1.12	1.65
(2c)	649 (115)	372, 326, 247	–	–	–

−2*J* value calcd. using the Bleaney–Bowers equation.

Table 2. Cyclic voltammetric and molar conductance data for the complexes in DMF

Complex	$E_{pc\ 1}$/V	$E_{pc\ 2}$/V	E_{pa}/V	Λ_m/S cm^2 M^{-1}
(1a)	−0.30	−0.95	−0.21	45
(2a)	−0.80	−1.81	1.23	46
(1b)	−0.80	−1.34	0.16	43
(2b)	−0.69	−1.16	−0.25	42
(1c)	−1.06	−1.31	−0.51	40
(2c)	−0.54	−0.77	−0.38	45

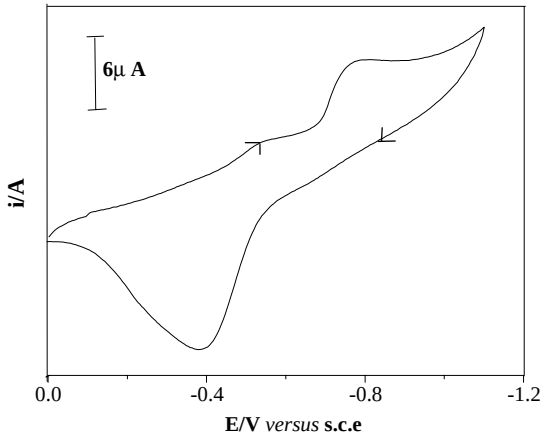

Fig. 2 Cyclic voltammogram of complex *(2c)*. Scan rate(v) = 50 mV s^{-1}.

changes after the first cycle. Two observed reduction peaks are assigned to stepwise reduction of the copper(II) ions. The first peak corresponds to the $Cu^{II}Cu^{II} \rightarrow Cu^{II}Cu^{I}$, and the second peak to $Cu^{II}Cu^{I} \rightarrow Cu^{I}Cu^{I}$. A broad anodic oxidation peak is observed for all the complexes in the −0.21 to 1.23 V range. The breadth of the oxidation peak suggests superposition of two close one-electron processes, which are assigned to the reoxidations of the $Cu^{II}Cu^{I}$ and $Cu^{II}Cu^{II}$ species, respectively. The irreversibility of redox processes in these complexes is attributed to changes in the coordination geometry or coordination number upon changing the oxidation state.

Magnetic studies

The observed room temperature magnetic moment values for the binuclear copper(II) complexes are in the 1.58–1.68 B.M. range, suggesting the presence of a weak antiferromagnetic interaction between the two copper(II) ions. To evaluate the singlet–triplet energy separation (−2J), variable temperature magnetic studies of the binuclear complexes were performed in the 80–300 K range and the experimental magnetic susceptibility values were fitted to the modified Bleaney–Bowers equation [11] to evaluate the best fit parameters for −2J, P and g.

$$\chi_m = \{Ng^2\beta^2/kT\}[3 + \exp(-2J/kT)]^{-1}(1 - P) + (Ngi^2\beta_t^2)/4kT)P + N_\alpha.$$

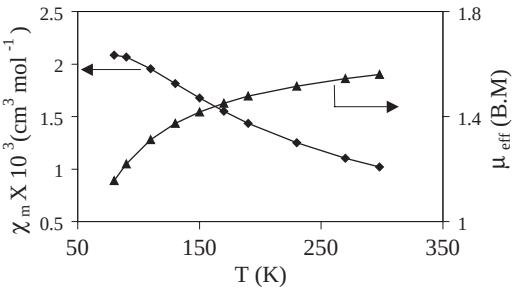

Fig. 3. Plots of the molar susceptibility per molecule (χ_m) *versus* temperature and of the effective magnetic moment per molecule (μ_{eff}) *versus* temperature for complex *(1c)*.

The value of N_α has been fixed as 60×10^{-6} cm^3 mol^{-1}. Here, χ_m is the molar magnetic susceptibility corrected for diamagnetism, and P is the percentage of paramagnetic impurities; the other symbols have their usual meaning. The magnetic parameters are also given in Table 1. Figure 3 depicts the temperature dependence of the magnetic properties of the complex *(1c)*.

Generally a weak exchange interaction is observed for unsymmetrical dicopper(II) complexes due to lack of coplanarity between the two copper planes [12, 13]. However other factors, *i.e.*, reduction in electron density on the copper atoms [14] and a distorted structure [15–19] are unfavorable for effecting coupling. In accordance with these results, the observed coupling constant values for the complexes are low. Comparison of the complexes *(2a*, *1b* and *1c)*, shows that the singlet–triplet splitting 2J varies systematically with coordination geometry about the $Cu_2O(X)$ core; the bromo and chloro bridged complexes exhibiting relatively high antiferromagnetic coupling compared to acetato bridged complexes. The extent of antiferromagnetic coupling increases in the order: $OAc^- < Cl^- < Br^-$. A lower −2J value observed for the acetato bridged complex is possibly due to the counter complementary nature of the overlap of the magnetic orbital involving the monoatomic and the three atom bridging ligands [20]. A slightly lower −2J value, observed for the chloro-bridged complex when compared to the bromo-bridged complex, may be due to the higher electronegativity of the former than of the latter.

Electron paramagnetic resonance studies

In order to gain further insight into the intramolecular magnetic interactions of binuclear copper complexes, X-band e.p.r. spectra were obtained for both powder and solution samples at 300 and at 77 K. The powder e.p.r spectra of $[Cu_2L(X)]^+$ complexes *(1a–2c)*, recorded at room temperature and at liquid N_2 temperature, show two different types of e.p.r. spectra. The complexes (*1a*), *(2a)*, *(2b)* and *(2c)* have broad isotropic spectral features, indicating the presence of an antiferromagnetic interaction [21] between the two copper(II) ions. On the other hand, bromo-*(1b)* and chloro-*(1c)* bridged complexes of H_2L^1 display axially symmetric spectra with

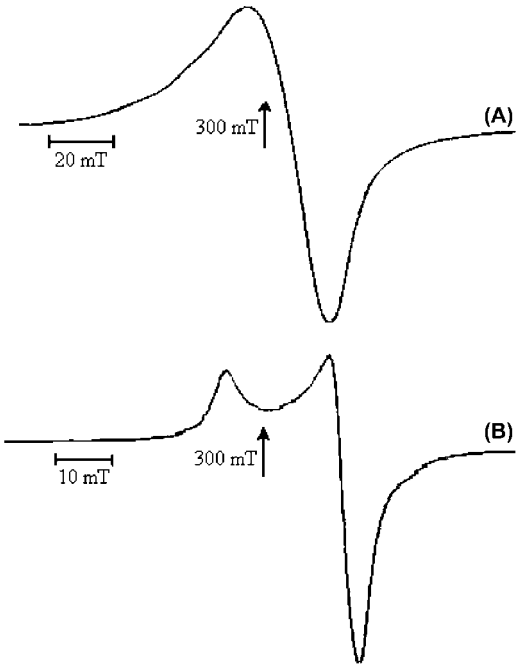

Fig. 4. X-band powder e.p.r. spectra at 77 K: (A) complex *(2a)*; $\nu = 9.03803$ GHz. (B) complex *(1c)*; $\nu = 9.03707$ GHz.

unresolved copper hyperfine resonances. This shows that the coupling between the two neighboring copper nuclei is reduced due to the presence of the electron-withdrawing bromo substituent at the *para* position of the phenolic ring, which reduces the electron density on the copper centre and consequently the effective overlap between the two metal orbitals. These features indicate that the complexes are antiferromagnetically coupled and that the exchange interaction is weak. These results reflect further the $2J$ values calculated from the variable temperature magnetic susceptibility measurements on powder samples. Typical powder e.p.r. spectra for the *(2a)* and *(1c)* complexes, recorded at 77 K, are given in Figure 4.

The room temperature solution e.p.r. spectra show the typical four-line pattern expected for coupling of the electron spin to the nuclear spin 3/2 of the copper nucleus. e.p.r. spectra of frozen solutions at 77 K are characterized by axial g and A tensors with $g_{\|} > g_{\perp}$ indicating the planar based geometry around the copper centre. Three of the four parallel hyperfine features are well resolved while the fourth one at high field is overlapped by the broad $g_{\perp}$ signal. These results indicate that the complexes undergo dissociation to a lesser extent by addition of coordinating solvent, and give spectra corresponding to the monomeric species [22].

All the e.p.r. parameters are given in Table 3. From the Table, we can see that the spin Hamiltonian parameters calculated from powder and solution spectra of complexes of H_2L^2, recorded at both RT and LNT, are almost similar but differ from complexes of H_2L^1. This shows that these complexes are sensitive to the (+ or −) inductive effect of the substituent on the phenyl ring and the exogenous bridges have little effect on these values. However, no final correlation can be drawn between these values and the intramolecular interaction between the two copper centres which is mainly tuned by the exogenous bridging nature as well as by the inductive effect of the phenyl ring substituent.

In order to confirm the spin Hamiltonian parameters, we have simulated a few powder and solution spectra using the e.p.r.-n.m.r. program [23] with the spin Hamiltonian parameters given in Table 3. The agreement between experimental and theoretical spectra is very good. A simulated and experimental e.p.r. spectrum of a liquid N_2 temperature DMF glass of complex *(1a)* is given in Figure 5.

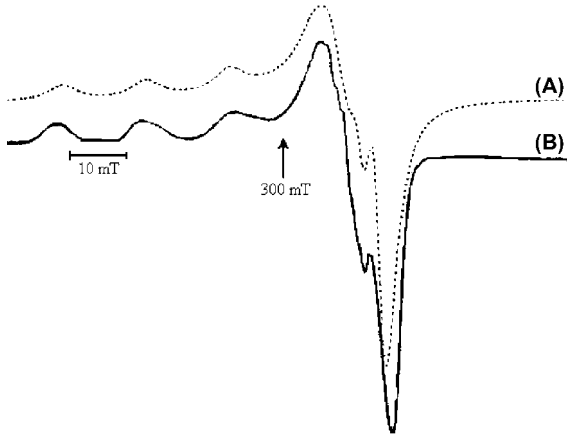

Fig. 5. X-band e.p.r. spectrum of a liquid N_2 temperature DMF glass of complex *(1a)*. (A) Simulated spectrum using the program e.p.r.-n.m.r. (B) Experimental spectrum. $\nu = 9.02785$ GHz.

Table 3. E.p.r. spectral data of the complexes (A values are in units of mT)

Complex	Powder		Solution (DMF)					
	300 K	77 K	300 K			77 K		
	g	g	g_{iso}	A_{iso}	$g_{\|\|}$	$g_{\|}$	$A_{\|\|}$	$A_{\|}$
(1a)	2.09	2.05	2.12	5.23	2.29	2.06	16.07	2.98
(2a)	2.10	2.09	2.12	6.72	2.28	2.04	15.60	2.53
(1b)	2.23[a], 2.08[b]	2.25[a], 2.09[b]	2.11	7.48	2.27	2.04	16.48	2.53
(2b)	2.09	2.08	2.11	7.06	2.26	2.04	16.60	2.33
(1c)	2.23[a], 2.08[b]	2.23[a], 2.08[b]	2.13	6.59	2.27	2.04	16.86	2.53
(2c)	2.07	2.07	2.11	6.72	2.26	2.04	17.07	2.33

$a = g_{\|}$; $b = g_{\perp}$.

Acknowledgements

P.S.R. thanks the DST, UGC, AICTE and CSIR {01(1771)/02/EMR-II} for financial support. R.M. thanks the CSIR (9/559 (026)/2000 EMR-I) for the award of a Senior Research Fellowship.

References

1. D.E. Fenton, in A.G. Sykes (Ed), *Advances in Inorganic and Bioorganic Mechanisms*, Academic Press, London, 1983, Vol. 2, p. 187.
2. T.N. Sorrell, *Tetrahedron*, **45,** 8 (1989).
3. J.D. Crane, D. E. Fenton, J.M. Lartour and A. Smith, *J. Chem. Soc., Dalton Trans.,* 2979 (1991).
4. W.P.J. Gaykema and W.G.H. Hol, *J. Mol. Biol.*, **209,** 249 (1989). W.P.J. Gaykema, A. Volbeda and W.G.H. Hol, *J. Mol. Biol.,* **187,** 2255 (1985).
5. J.K. Lerch, M. Huber, H.J. Schneider, R. Dresel and B. Linzen, *J. Inorg. Biochem.*, **26,** 213 (1986).
6. D.D. Perrin and W.L.F. Armarego, *Purification of Laboratory Chemicals*, 3rd edit., Pergamon Press, New York, 1988.
7. E.W. Ainscough, A.G. Bingham, A.M. Brodie, J. Husbands and J.E.J. Plowman, *J. Chem. Soc., Dalton Trans.*, 1701 (1981).
8. R.C. Holz, J.M. Brink, F.T. Gobena and C.J. O'Conner, *Inorg. Chem.*, **33**, 6086 (1994).
9. K. Nakamoto, *Infrared and Raman Spectra of Inorganic and Coordination Compounds*, 3rd edit., Wiley, New York, 1978, p. 232.
10. R.E. Dessy, P.M. Weissman and R.L. Pohi, *J. Am. Chem Soc.*, **88**, 117 (1996).
11. B. Bleaney and K.D. Bowers, *Proc. R. Soc. Lond. Ser. A*, **214**, 451 (1952).
12. D.J. Crame, D.E. Fenton, J.M. Latour and A. Smith, *J.Chem. Soc., Dalton Trans.*, 2979 (1991).
13. A Benzekri, P. Dubourdeaux, J.M. Latour, J. Laugier and P. Rey, *Inorg. Chem.*, **27**, 3710 (1988).
14. L.K. Thomson, S.K. Mandal, S.S. Tandon, J.N. Bridson and M.K. Park, *Inorg. Chem.*, **35,** 3117 (1996).
15. Y. Nishida, H. Shimo, H. Maehara and S. Kida, *J. Chem. Soc., Dalton Trans.*, 1945 (1985).
16. T.N. Sorrell, D.L. Jameson and C.J. O'Conner, *Inorg. Chem.*, **23,** 190 (1984).
17. L. Lorosch and W. Hasse, *Inorg. Chim. Acta*, **108,** 35 (1985).
18. M. Handa, N. Koga and S. Kida, *Bull. Chem. Soc., Jpn.*, **11,** 3853 (1988).
19. H. Astheimer and W. Hasse, *J. Chem. Phys.*, **85**, 1427 (1986).
20. K. Geetha, M. Nethaji, A.R. Chakravarthi and N.Y. Vasanthacharya, *Inorg. Chem.*, **35**, 7666 (1996).
21. R.C. Agarval, N.K. Singh and R.P. Singh, *Inorg. Chem.*, **20,** 2794 (1981).
22. M.M. Whittaker, W.R. Duncan and J.W. Whittaker, *Inorg. Chem.*, **35**, 382 (1996).
23. EPR-NMR program developed by F. Clark, R.S. Dickson, D.B. Fulton, J. Isoya, A. Lent, D.G. Mcgavin, M.J. Mombourquette, R.H.D. Nuttall, P.S. Rao, H. Rinneberg, W.C. Tennant and J.A. Weil, University of Saskatchewan, Saskatoon, Canada (1996).

TMCH 5891